Possible mechanisms for protecting NCα bonds in helical peptides from electron-capture (or transfer) dissociation

ARTICLE · SEPTEMBER 2007

DOI: 10.1016/j.ijms.2007.02.001

4 AUTHORS, INCLUDING:

Piotr Skurski
University of Gdansk
140 PUBLICATIONS **3,382** CITATIONS
SEE PROFILE

Jacek Jakowski
University of Tennessee
38 PUBLICATIONS **470** CITATIONS
SEE PROFILE

Available online at www.sciencedirect.com
ScienceDirect
International Journal of Mass Spectrometry 265 (2007) 197–212
International Journal of Mass Spectrometry
www.elsevier.com/locate/ijms

Possible mechanisms for protecting N–C_α bonds in helical peptides from electron-capture (or transfer) dissociation

Piotr Skurski [a], Monika Sobczyk [a], Jacek Jakowski [b], Jack Simons [a,*]

[a] *Department of Chemistry and Henry Eyring Center for Theoretical Chemistry, University of Utah, Salt Lake City, UT 84112, United States*
[b] *Chemistry Department, Indiana University, Bloomington, IN, United States*

Received 3 October 2006; received in revised form 26 January 2007; accepted 7 February 2007
Available online 11 February 2007

Abstract

Ab initio electronic structure simulations are carried out on small alanine-based peptide fragments with an excess electron added to a Coulomb-stabilized amide OCN π* orbital that forms a $^{\bullet}C{-}O^{-}$ radical anion center. A focus of the study is to determine to what extent and by what means helix-involved N–C_α bonds are "protected" against cleavage compared to similar bonds in non-helical peptides. The primary findings, many of which support earlier suggestions, include:

(1) There is little or no increase in the energy barriers for N–C_α bond cleavage caused by an amino acid being in a helix where its carbonyl oxygen is involved in a hydrogen bond to an H–N bond of an amino acid displaced by one helix turn.
(2) When an electron attaches to a helix-involved Coulomb-stabilized OCN π* orbital and the N–C_α bond cleaves, three hydrogen bonds act to bind together the c and $z^{\bullet}$ fragment ions. One of these hydrogen bonds is especially strong (ca. 16 kcal mol^{-1}) because it involves a negatively charged oxygen center. This suggests that the "protection" against N–C_α cleavage of helix-involved amino acids may, as others suggested earlier, result from the strong hydrogen bonding that binds the c and $z^{\bullet}$ fragment ions.
(3) When an electron attaches to a helix-involved OCN π* orbital, an electron can migrate to the π* orbital of another amino acid one turn down the helix, but only by overcoming a barrier. After migrating to a new amino acid, N–C_α cleavage can occur at the latter site, also in line with what earlier workers have suggested.

Suggestions of experiments that might test the hypotheses treated here are also put forth.

Keywords: Alpha helix; N–C alpha cleavage; Electron capture dissociation; Electron transfer dissociation; Coulomb stabilization

1. Introduction

It has been found that disulfide and amide N–C_α bonds in proteins and peptides are likely to be ruptured when low-energy electrons attach to positively charged samples of these species in electron-capture dissociation [1] (ECD) or electron-transfer dissociation [2] (ETD) mass spectrometric experiments. However, the mechanisms by which the attached electron induces such cleavages have not yet been fully characterized although much progress has been made [3] toward this end.

The present paper attempts to provide further insight into these mechanistic issues particularly for species containing helical subunits. Before discussing the issues that arise in helices, it is useful to briefly review the three classes of mechanisms that have been suggested to contribute to electron-induced ETD and ECD disulfide (S–S) linkage and N–C_α bond cleavage. In ECD and ETD samples, the molecule to which the electron attaches is positively charged and usually has more than one positive site (e.g., protonated amine sites on side chains). Subsequent to electron attachment to such a sample, bond cleavage may occur and fragment ions can form and be detected. One of the strengths of ECD and ETD is that many N–C_α bonds along the backbone are observed to cleave, so a wide range of product ions are obtained thus giving much sequence information.

* Corresponding author. Tel.: +1 801 581 8023.
E-mail address: simons@chemistry.utah.edu (J. Simons).

1387-3806/$ – see front matter © 2007 Elsevier B.V. All rights reserved.
doi:10.1016/j.ijms.2007.02.001

Of course, the determination of the identities and abundances of the fragment ions is a key ingredient in the use of ECD or ETD to determine primary sequences of peptides and proteins. Although there are differences noted in the abundances of various fragment ions obtained using ECD or ETD, both procedures give substantial S–S and N–C_α cleavage, and both are thought to proceed through similar mechanisms. Therefore, in the present paper, we will not discuss the differences between ECD and ETD; rather, we will focus on what happens once an electron has was captured, regardless of whether it attached or was transferred.

1.1. Alternative mechanisms

1.1.1. The Cornell hydrogen atom mechanism

The earliest proposed mechanism, suggested by McLafferty and Zubarev [1a] at Cornell, posits that electron attachment occurs at a protonated site (that is probably hydrogen bonded to a nearby carbonyl oxygen or to a S–S unit) to form a hypervalent radical. This radical subsequently transfers an H atom to the nearby carbonyl or SS unit to form a radical that either undergoes prompt S–S bond rupture or facile N–C_α bond cleavage. This mechanism is described in Scheme 1 where the c/z$^\bullet$ notation used to describe the fragments produced by N–C_α cleavage is also illustrated and color is used to focus on the part of the molecule where the electronic "action" is taking place. The wavy lines shown in this and other schemes are intended to represent backbone and side chain units separating the charged site and the OCN or SS functional group; there may be one or several amino acids separating the SS or OCN group and the charged site, but in the present mechanism, the charged site must be close enough to effect H atom transfer once an electron attaches to the positive site.

A key to the mechanism shown in Scheme 1 is that a hydrogen atom is what attacks the S–S σ or C=O π bond to initiate the cleavage process.

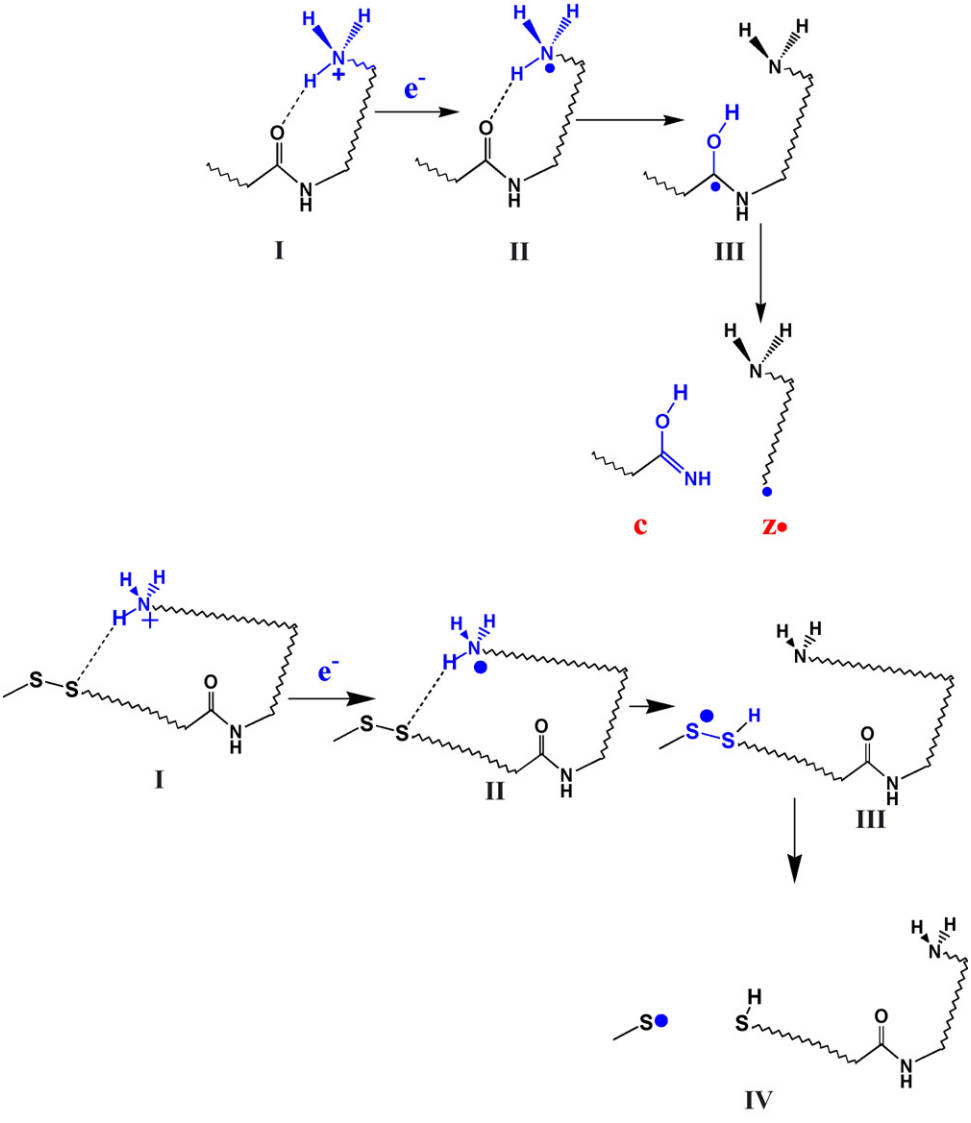

Scheme 1.

1.1.2. The Coulomb-stabilized direct attachment mechanism

The second class of proposed mechanism that our group and that of Turecek have proposed [3j,3f,3l,3m] does not require that the positively charged site be within a hydrogen bond length of the S–S or carbonyl unit nor does it require that the positive site involve protonation. It posits that the Coulomb potential [4] provided by positive site(s) can lower the energies of the S–S σ* and amide OCN π* orbitals (relative to their energies in the absence of Coulomb stabilization) sufficiently to render exothermic the direct electron attachment to either of these orbitals.

After electron attachment to an S–S σ* orbital, the S–S bond promptly ruptures forming an R–S$^{\bullet}$ radical and an $^{-}$S–R′ negative center. Then, proton transfer may (but not necessarily) occur to neutralize the negative center. Alternatively, when an electron is attached to an OCN π* orbital, the energy required to break the N–C_{α} bond is reduced by the ability of the π* anion center to subsequently form a new C=N π bond as shown in Scheme 2. Upon N–C_{α} cleavage, a carbon-centered radical and a negatively charged $^{-}$O–C=NH center are formed. Subsequent transfer of a proton (e.g., from a protonated amine site) may (but not necessarily) occur to neutralize the latter to form either a HO–C=NH unit (as in Scheme 1) or the more stable O=C–NH_2.

A key to this mechanism is that it is an electron that attacks the S–S or OCN unit (attaching to the SS σ* or OCN π* orbital) with proton transfer (possibly) occurring after bond cleavage. Another key is that the potential proton transfer need not come from a site that had been in close contact with the S–S or OCN group. It can come from further away and from either the C- or N-terminal side, although, of course, the Coulombic attraction to the nascent negative site would tend to induce proton transfer from a nearby positive site.

Direct vertical electron attachments to an S–S σ* or OCN π* orbital are known [5] to be ca. 1 eV and 2.4 eV endothermic, respectively, in the absence of Coulomb stabilization. So, this mechanism is not expected unless there are positively charged groups sufficiently nearby. However, even a single positively charged site located ca. 14 Å (for the S–S σ* orbital) or ca. 6 Å (for the amide π* orbital) from the bond to be broken can be expected to be capable, according to this mechanism, of effecting bond cleavage.

In [3h,3i] we showed that the cross-sections for electron transfer to OCN π* or S–S σ* orbitals can be expected to be one to two orders of magnitude smaller than for transfer to a Rydberg orbital of a positively charged site (e.g., a –NH_3^+ site). This suggests that, if the positive site is not closely associated (e.g., hydrogen bonded) with the S–S or carbonyl oxygen site, most of the bond cleavage can occur via the Coulomb-assisted direct attachment path even though most of the electrons may be transferred to the positive site. We should note that our electron transfer studies should be viewed as representative of ETD conditions and may not be equally applicable to ECD, although we see no reason to expect the conclusions we reached to not be applicable to both conditions. There remains much work to be done to more fully address the branching ratios for attachment or transfer to various Rydberg levels of positive sites and for transfer from one positive site to another, and we are presently undertaking such studies.

1.1.3. The intramolecular electron transfer mechanism

The third mechanism class that we have also proposed [6] suggests that the electron initially attaches to a positively charged site, which need not be within hydrogen-bonding distance of the S–S or OCN unit, initially to form an excited-state hypervalent (also called Rydberg) species. This excited state can then undergo relaxation (non-radiative or radiative) to lower Rydberg states. Subsequently, a through-bond electron transfer (TBET) from one of the Rydberg orbitals of the hypervalent species to either the S–S σ* or OCN π* orbital takes place, after which cleavage of the S–S or N–C_{α} bond can occur much as in Scheme 2. This mechanism is illustrated for the N–C_{α} cleavage case in Scheme 3 (the mechanism for S–S cleavage should be clear from Schemes 2 and 3).

Note that the same fragment species occur in Scheme 3 as in Scheme 2 and that the final proton transfer step may or may not occur (i.e., is not necessary to realize bond cleavage).

1.2. Observations to compare the three mechanisms

A few observations that may distinguish among the three proposed mechanisms are useful to keep in mind because they may guide future experimental efforts aimed at determining which mechanism is most important under various circumstances.

(1) As noted above, Scheme 1 generates only the HO–C=NH unit (i.e., not O=C–NH_2) upon N–C_{α} cleavage, whereas Schemes 2 and 3 may (but not necessarily) generate either. Moreover, in Scheme 1, a negative $^{-}$S–R or $^{-}$O–C=NH unit is not generated, whereas in Schemes 2 and 3 such negative centers can arise and persist if proton transfer does not take place after bond cleavage (e.g., if the positively charged sites are not protonated and if there are no nearby labile proton sources). These differences are not possible to detect from mass-to-charge ratio measurements, but any method to probe them could help guide us in determining, which schemes are operative.
(2) The mechanism of Scheme 1 requires that the amide carbonyl or SS bond and the positively charged site be within hydrogen-bonding distance of one another. This suggests that bond cleavage should occur only within amino acids proximal to positively charged side chains (although, as we discuss later in Section 4.3 and as others have suggested, –OC(•)–N radical propagation steps within this mechanism could explain cleavage at more distant amino acids). Even if the bond and positive sites do not have to be close enough to form an intact hydrogen bond, geometrical considerations [7] suggest that the effectiveness of this process should decay as R^{-2}, where R is the distance between the two sites, because it requires an H atom to be transferred between the two sites. This mechanism also requires that the positive site generate an H atom upon attaching an electron, so species with fixed positive charges (e.g., –$N(CH_3)_3^+$ units) should not produce cleavage within this mechanism.

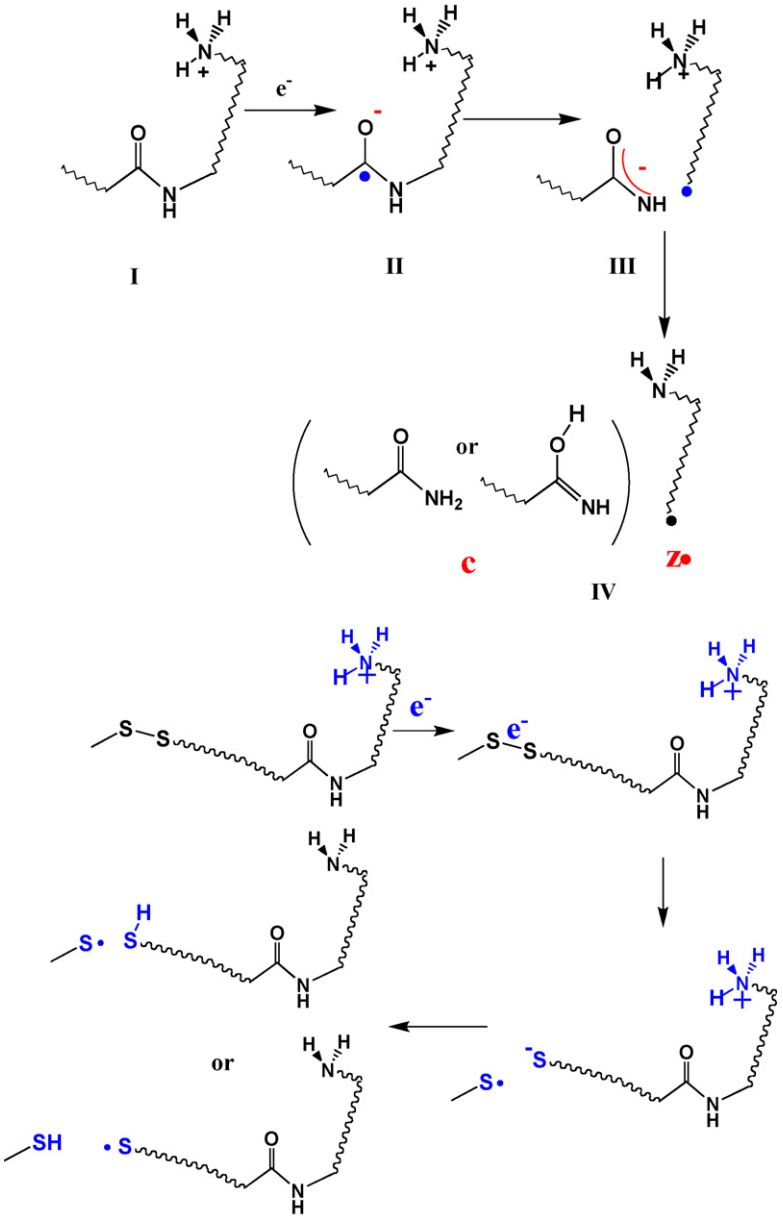

Scheme 2.

(3) The direct Coulomb-assisted electron attachment mechanism would be expected to allow bond cleavage whenever the bond and positive sites are close enough for the Coulomb potential [4,8] 14.4 eV Å/R(Å) to exceed the σ* or π* orbital's intrinsic attachment endothermicity [5] ΔE (ca. 1 eV for S–S σ* and ca. 2.4 eV for amide π* orbitals). For distances R greater than R_C = 14.4 eV Å/ΔE (eV), this mechanism should be quenched. This mechanism should also be expected to occur when positive sites involve fixed charges and in the absence of nearby labile proton sources.

(4) The through-bond electron transfer mechanism's efficiency should decrease exponentially (i.e., as exp(-βR)) with the distance R between the bond and positive sites. In [6] we determined the exponential decay constant β (ca. 1 Å^{-1}) for cases in which the attached electron migrates through saturated units such as –CH_2– groups (see also [11] for discussion of how β is obtained and what it means). It may be that the rates at which electrons can undergo through-bond transfer from a Rydberg orbital through peptide bonds is qualitatively different; we are currently considering this.

Later in this paper, we make use of these observations about the three mechanistic options to suggest experimental tests by which one can distinguish further among these possibilities.

2. Suggestive experimental evidence on model helical peptides that also contain a disulfide linkage

Although the emphasis of this paper is on N–C_α cleavage in helical peptides, a few examples from the recent experimental literature pertaining to peptides containing both N–C_α and disulfide linkages and containing protonated and fixed-charged

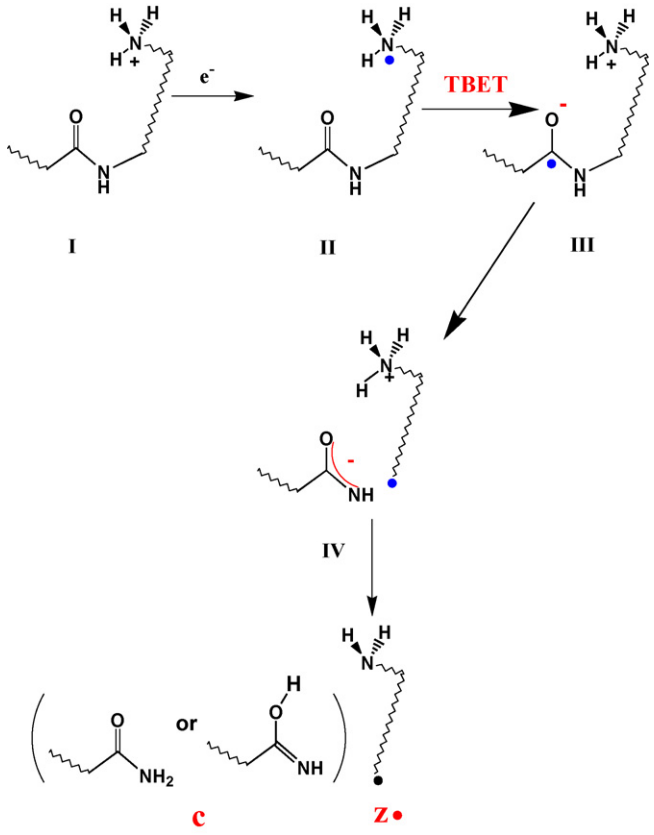

Scheme 3.

positive sites are useful to discuss first because they shed considerable light on how the mechanisms shown in Schemes 1–3 are likely to contribute and they justify our decision to focus on the mechanism shown in Scheme 2 in the present treatment of N–C_α cleavage within helices.

2.1. S–S bond cleavage can be observed even when protonated amine sites are 30 Å away

Recent experimental studies are discussed in [3j] on ECD cleavage of synthetic disulfide linked systems including $(AcCA_nK+H)_2^{2+}$, with $n=10$, 15, and 20 that are protonated at the terminal Lys sites. These data were obtained by Hudgins while in the Marshall group, have been presented in public at meetings, but have only appeared in print in a joint paper ([3j]) by Hudgins and this author's group.

Because the Ala_n units in $(AcCA_nK+H)_2^{2+}$ are expected to adopt a helical extended structure as shown in Fig. 1, one expects the distance between the charged Lys sites to grow monotonically with n. Moreover, ion mobility measurements [9] supported the assumed extended quasi-linear structure for this species. Nevertheless, in the studies described in [3j], significant S–S cleavage was observed even for the $n=20$ system in which the S–S bond is thought to be ca. 32 Å from either protonated Lys. If the first mechanism described above were the only one operative, one would expect the yield of S–S cleavage to greatly decrease as n increases because the ability of the H atom to reach the disulfide linkage should decay with distance.

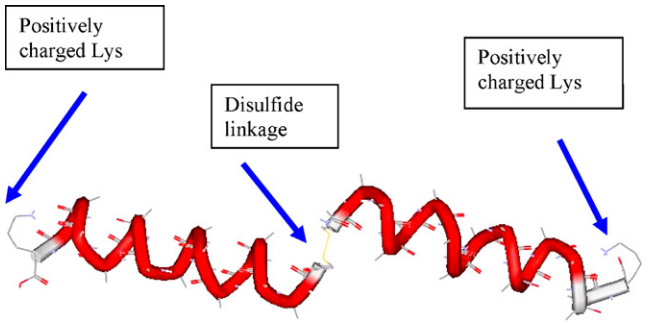

Fig. 1. Assumed structure of the $(AcCA_{15}K+H)_2^{2+}$ disulfide-linked dimer (slightly redrawn from what appears in [3j]). The disulfide linkage is at the center and the two charged Lys sites are at the left and right ends as shown by arrows.

Specifically, for $n=20$, it is difficult to imagine how an H atom released from one of the Lys termini could make its way to and cleave the disulfide linkage.

On the other hand, we note that the Coulomb potential generated at the disulfide linkage site by the two positively charged Lys units in the $n=20$ species would be approximately 2×14.4 eV Å/32 Å or ca. 1 eV, just enough [5] to render operative the direct attachment to the S–S σ* orbital as in the second mechanism introduced in Section 1. We also note that the substantial amount of S–S cleavage observed as n varied from 10 to 20 also argues against the through-bond electron transfer mechanism [10,11], at least for the system shown in Fig. 1. The efficiency of the through-bond electron transfer mechanism should decay rapidly [11] (exponentially) as n increases and, as noted earlier, the effectiveness of the first mechanism should also decay inversely with the distance between the SS bond and the positive charges. Thus, at least for the $n=20$ species, both the through-bond and the hydrogen atom mechanism should be questioned.

2.2. S–S bond cleavage occurs even when the amine sites are alkali-ion charged

Further useful evidence [12] was provided from experiments (also see [3j]) on very similar S–S bond containing synthetic peptides (e.g., $AcCA_{10}–NH_2+Na)_2^{2+}$ that were charged with Na^+ cations (presumably on the C-termini) instead of protons. The ECD data on these samples also showed substantial fragmentation of the S–S bond, thus suggesting that transfer of an H atom from a hypervalent site to the S–S bond is not necessary. We should mention that our calculations show that removal of an H atom from a $–NH_2Na$ site (i.e., a sodiated amine site to which an electron has attached) is ca. 70 kcal mol^{-1} endothermic, whereas removal of a Na atom requires only ca. 7 kcal mol^{-1}. Thus, as suggested in [3j], it is unlikely the sodiated species have labile hydrogen atoms that could play the role necessary for the first mechanism of Section 1 to be operative. Moreover, any neutral Na atoms released after electron capture (or attachment) would not be expected to cleave the S–S bond. So, one is left wondering how S–S cleavage occurs in these alkali-charged systems other than by the second mechanism.

2.3. N–C_α cleavage can occur when labile H atoms are not present

In [12], N–C_α bond cleavage data was also reported under ECD conditions for other species charged using alkali cations instead of protons [e.g., $(LHRH + 2Na)^{2+}$], of peptides with fixed charges [$(Ac–Kbt–Gly_5–Kbt–NH_2)^{2+}$], and of peptides devoid of labile hydrogens [$(Ac–Sar_{15}–OMe + 2Na)^{2+}$]. In these samples, substantial N–C_α bond cleavage was observed and the corresponding c/z$^\bullet$ fragments were found. These findings as well are difficult to reconcile with Scheme 1, which requires an H atom to attack the OCN unit to generate the c and z$^\bullet$ fragments.

2.4. Only N–C_α cleavage near the charged Lys termini occurs in helices

In the ECD fragmentation of $(AcCA_nK + H)_2^{2+}$ and $(AcCA_{10}K + Na)_2^{2+}$, certain c and z$^\bullet$ fragment ions have also been observed [3j]. The c/z$^\bullet$ backbone fragmentation in $(AcCA_{15}K + H)_2^{2+}$ and $(AcCA_{20}K + H)_2^{2+}$ is limited to the four C-terminal amino acids. It was suggested that these findings occur because these four amino acids are exposed to (i.e., geometrically accessible to) the positively charged Lys. In $(AcCA_{10}K + H)_2^{2+}$, N–C_α cleavages again occur at the four C-terminal amino acids, but also slight cleavage of the next three amino acids is seen, which has been taken to indicate some fraying of this helix in this species. It was also suggested that the amino acid units further from the C-termini, where c/z$^\bullet$ fragmentation is not observed, have their carbonyl oxygen atoms involved in helix ···H–N hydrogen bonds that "protects" these units against N–C_α cleavage. Furthermore, it was noted in [3j] that ECD of $(AcCG_{10}K + H)_2^{2+}$ (i.e., with alanine replaced by glycine thereby presumably eliminating the helical structures), produced N–C_α cleavage throughout the entire backbone, again suggesting that it is the helical structure that somehow forbids N–C_α cleavage except within four amino acids of the C-terminus.

The body of data discussed above is suggestive that Scheme 1 alone may not be operative, and it is at least as supportive of Scheme 2 as it is of any other option. However, the findings pertaining to N–C_α cleavage at some, but not all, sites within helical structures require further study. To us, it is by no means clear what the physical mechanism is by which involvement in a helical hydrogen bonding network protects OCN units against attack either by H atoms (the first mechanism in Section 1) or by electrons (the second and third mechanisms). Also, it is not clear that the four amino acids closest to the protonated (or sodiated) Lys sites discussed above are susceptible to N–C_α cleavage (only) because they may not be involved in the helical structure. As an alternative, we suggest that the amino acids closest to the C-termini may be close enough to the charged Lys sites to undergo the direct Coulomb-assisted electron attachment of Scheme 2 and this is why they are found to produce c/z$^\bullet$ fragments. Let us now turn to discuss the strategy and computational methods used to address this suggestion and others.

2.5. Strategy and questions to be addressed

Because of the above questions about the role of the helix in protecting certain N–C_α bonds, we decided to carry out a series of ab initio electronic structure simulations designed to consider:

(1) What can happen when an electron attaches to a Coulomb-stabilized OCN π^* orbital within a model α-helical peptide (n.b., we focus our treatment on the mechanism of Scheme 2 given the data discussed earlier that seem to support it over the other two schemes).
(2) Whether an electron attached to the OCN π^* of one amino acid could migrate to another amino acid one turn displaced along the helix.

Among the specific possibilities we wanted to consider were:

(1) That the barrier to N–C_α cleavage in a helical system could be increased, over that arising in the absence of helical structure, by the O···H–N hydrogen bonds that connect the carbonyl oxygen and amide H–N centers and that this could be the means of "protecting" helix-involved N–C_α bonds.
(2) That cleavage of the helix-involved N–C_α bonds can occur with little or no additional barrier, but that the three hydrogen bonds still connecting the N–C_α bond-cleavage product ions are, in combination, strong enough to preclude dissociation of the c and z$^\bullet$ products under typical ECD conditions. Of course, if this is the case, it suggests that ECD or ETD followed by collisionally activated decomposition (CAD) should generate the separated c and z$^\bullet$ fragments.
(3) That an electron attached to one OCN π^* orbital might be propagated along the helix through the hydrogen bond network to an OCN π^* orbital of another amino acid thus allowing N–C_α bond cleavages to occur at sites other than that to which the electron initially was attached.
(4) That the tendency of N–C_α bonds within four amino acid units of the C-terminus to cleave may be due either to Coulomb-assisted direct electron attachment (Scheme 2) to these amide sites (which are close to a positive charge) or to electron migration from one amide π^* orbital to another following direct attachment near the C-terminus.

Although we leave a more detailed discussion of our findings on these topics to Sections 4.3, 4.4 and 5, we should note that others have earlier suggested that hydrogen bonding may be what holds together incipient c/z$^\bullet$ fragments and that radical propagation along helices can indeed occur thus allowing c/z$^\bullet$ cleavage distant from the site of electron attachment. However, the present paper offers, we believe, a more quantitative picture of these events and their influence on N–C_α cleavage within helices.

3. Methods

To address the issues discussed above, we decided to investigate model structures representative of helical alanine systems

each of which allows us to examine N–C_α bond cleavage as well as migration of the attached electron subsequent to direct electron attachment.

The first model system consists of only two alanine units positioned relative to one another to simulate the spatial arrangement of two hydrogen-bonded units within a helical structure. The idea of creating this small two-alanine system is based on the desire to model the helix structure in as simple as possible a manner (in order to simplify the ab initio calculations carried out) while preserving a main characteristic of helical units (i.e. hydrogen bonds stabilizing the secondary structure). The second model system consists of a chain of five alanines arranged into an α-helix structure.

All calculations were carried out within an ab initio theoretical framework based on unrestricted Hartree–Fock (UHF) and second-order Møller–Plesset (MP2) levels of theory using 6-31G(d) basis sets [13]. In addition, a stabilizing Coulomb potential was included to simulate the presence of nearby positively charged groups that act to lower the energy of the amide π* orbitals thus allowing direct electron attachment followed by N–C_α bond rupture or π*-electron migration.

Because of the size of these molecules, and considering the large number of geometries at which we needed to evaluate the energies, we first partially optimized the geometries of both systems at the Hartree–Fock self-consistent (SCF) level of theory with some geometrical variables frozen (to retain helical structural aspects) while relaxing the other degrees of freedom to minimize the electronic energy. We chose to relax the variables (i.e., bond lengths and valence or dihedral angles) essential to describe breaking the S–S and N–C_α bonds within the investigated model compounds. For example, in cleaving an N–C_α bond, we need to allow for changes in the local hybridization, bond lengths, and angles (i.e., geometrical structure) around the nitrogen and carbon atoms as well as for the oxygen atom involved in the OCN unit.

We subsequently repeated our UHF-level evaluations of the energies at the second-order Møller–Plesset (MP2) correlated level of theory to gain more accurate estimates of the bond-cleavage energy profiles. In order to generate our final energy profiles as functions of various bond lengths, we performed MP2 calculations at a range of bond lengths with all geometrical degrees of freedom frozen at the values they have in the SCF-computed structures.

Because the methods we used are based on an unrestricted Hartree–Fock starting point, it is important to make sure that little if any artificial spin contamination enters into the final wave functions. The unrestricted calculations were necessary to achieve a qualitatively correct description of the homolytic cleavage of the bonds and because some of the molecules we analyzed are open-shell species. We computed the expectation value $\langle S^2 \rangle$ for all species studied in this work and found values not exceeding 0.77 (after annihilation) for doublets. The Gaussian 03 suite of programs [14] was used to perform all of the calculations, and the Molden visualization program [15] was employed to examine the molecular orbitals and to construct some of the molecular structures shown.

4. Results

4.1. N–C_α bond cleavage of amide π*-attached anions with and without hydrogen bonding

Throughout this paper, we will refer to the amino acid whose amide H–N bond is hydrogen-bonded to a given amino acid's carbonyl oxygen as the "neighboring" amino acid recognizing, of course, that, in a helix, these two amino acids are not connected along the backbone but, instead, are displaced by four amino acids. That is, we define the helical neighbor of the *i*th amino acid as the $(i+4)$th amino acid.

In presenting and discussing our results, we first offer data obtained on a single alanine and on two alanines positioned with one amino acid's carbonyl oxygen atom hydrogen bonded to the H–N bond of a second amino acid positioned in a manner to simulate the orientation of two amino acids in a helix. We offer data on the barrier to N–C_α bond cleavage for the single-alanine model system as well as data showing how an electron initially attached (subject to Coulomb stabilization) to the OCN π* orbital of one amino acid might migrate down the helix to another amino acid. Subsequent to discussing our findings on these one- and two-amino-acid model systems, we present analogous data on a larger model system consisting of five alanines arranged in a helix.

We present in Fig. 2a the reaction energy profile for N–C_α cleavage of the smallest model compound in which:

(a) An electron is attached to the OCN π* orbital of a single alanine.
(b) A positive charge (to simulate the Coulomb stabilization of a nearby charged group) has been placed (as shown in Fig. 2a) in close enough proximity to the OCN unit to render electron attachment to this π* orbital exothermic.
(c) The N–C_α bond is elongated enough to allow the π*-attached electron to migrate onto the N–C σ* orbital and thus effect N–C_α cleavage.

In Fig. 2b, analogous energy profiles are shown for a species with an electron attached to an alanine whose carbonyl oxygen is hydrogen bonded to an H–N bond of a nearby methyl amine.

The key features to note in the data shown in Fig. 2 are as follows:

(1) In both cases, as the N–C_α bond is elongated and begins to undergo homolytic cleavage, an intersection between the π*-attached and σ*-attached electronic states occurs at an energy of ca. 30–34 kcal mol^{-1}. At this crossing, the attached electron can migrate from the π* orbital into the N–C σ* orbital and effect bond cleavage. The energy of this curve crossing (30–34 kcal mol^{-1}) is significantly lower than the dissociation energy of a typical N–C σ bond because of the concerted formation of a π bond between the nitrogen atom and the carbonyl carbon atom that takes place once the N–C_α bond breaks (see Scheme 4).

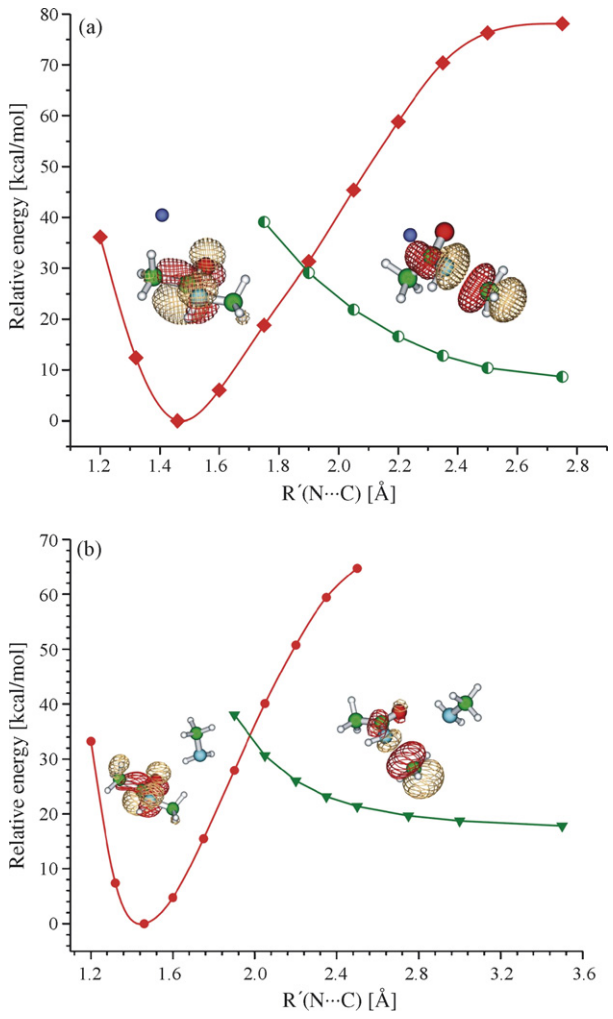

Fig. 2. (a) (Top): MP2-level energies of Coulomb-stabilized alanine π*-attached (red) and N—C_α σ*- attached (green) electronic states as functions of the N—C_α bond length; (b) (bottom): similar plots but with the carbonyl oxygen involved in a hydrogen bond to a neighboring H—N bond of methyl amine. Also shown are the orbitals holding the excess electron for each state.

(2) The barrier to cleave the N–C_α bond (ca. 30 kcal mol^{-1}) in alanine itself is not substantially different from that for cleavage of the N–C_α bond when the alanine is involved in hydrogen bonding to a nearby amine (34 kcal mol^{-1}).

(3) These barriers are similar to those that have been found by Turecek [16] for N–C_α cleavage (with and without involvement in ···H–N hydrogen bonding) in studies of the first mechanism discussed above (Scheme 1) that involve a R–C•(OH)–NHR' carbon radical fragmenting to form R–C(OH)=NH + •R′. They are also similar to those found at a higher level of theory (102 kJ mol^{-1} or ca. 24 kcal mol^{-1}) by Turecek in [3f] where a point charge at a different location was used to stabilize direct electron attachment to the amide π* orbital much as we consider here for the mechanism of Scheme 2.

(4) For the alanine-plus-methyl amine case shown in Fig. 2b, following N–C_α cleavage, an ion–molecule complex is formed in which a hydrogen bond connects the amine and the negatively charged oxygen atom of the carbonyl group. To subsequently break this hydrogen bond and dissociate this Me–O^-–C=NH···H_2N–Me complex requires > 16 kcal mol^{-1}. As we show later in Section 4.4 for a five-alanine model helical system, such a negatively charged oxygen center cannot abstract a proton from the H–N bond to which it is hydrogen bonded. In the case shown in Fig. 2b, it is endothermic to abstract a proton from H_2N–CH_3 and in the five-alanine case, it is endothermic to abstract a proton from the amino acid to which this negative oxygen is hydrogen bonded.

The above anion-centered hydrogen bond merits further discussion. The strength of the hydrogen bond between the amine and the oxygen-centered anion is large (>16 kcal mol^{-1}) because it involves a negative ion. We suggest that this strong hydrogen bond, combined with the two other (conventional ca. 5 kcal mol^{-1}) hydrogen bonds that arise in every helix turn, may act to inhibit separation of the c and z• fragment ions formed when N–C_α bond cleavage takes place. This > 16 + 5 + 5 = 26 kcal mol^{-1} barrier to c/z• fragment separation could be at least part of the source of "protection" that helix-involved N–C_α bonds appear to possess (as others have suggested (see Sections 4.3 and 5). That is, these findings suggest that N–C_α cleavage actually occurs in helices but the c/z• fragment ions are simply held together by strong hydrogen bonding and thus not detected unless subjected to subsequent collisional (or other) activation.

4.2. Migration of the π*-attached electron along the helix

In Schemes 5 and 6, we show two means by which a site of potential N–C_α cleavage, initially caused by attachment of

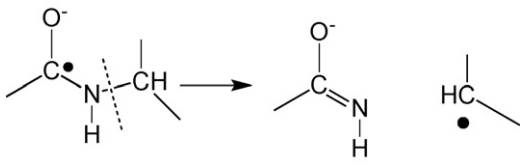

Scheme 4.

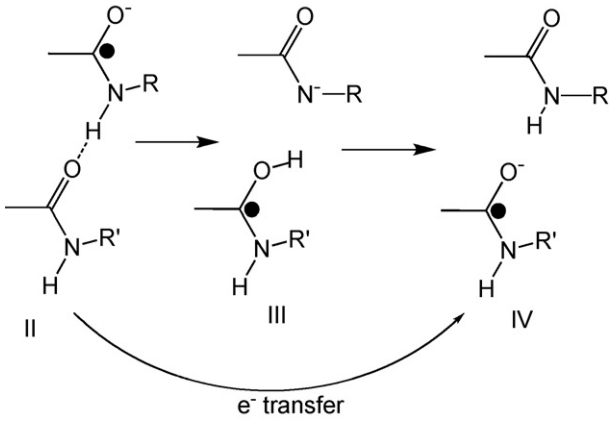

Scheme 5.

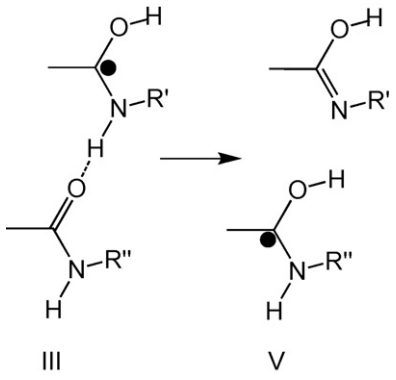

Scheme 6.

an electron to an amide π* orbital, might be able to propagate from one amino acid to another along a helix. These processes involve displacements of nuclei in the molecular framework accompanied by rearrangements in the orbital occupations of the electrons, so they are difficult to represent by the conventional electron pushing arrows one sees in textbooks. Let us now explain the geometry and electronic changes involved in these propagation steps.

In Scheme 5, an electron initially in a C=O π* orbital on the top amino acid (thus generating the •C–O⁻ radical anion center II of Scheme 2) moves into the N–H σ* orbital as the N–H bond elongates. This cleaves the N–H bond to leave the nitrogen center negatively charged and to release an H atom. This H atom attacks the π bond of the oxygen of the carbonyl group to which is had been hydrogen bonded to form a covalent H–O bond and generate a (neutral) •C–OH radical center III. Finally, the

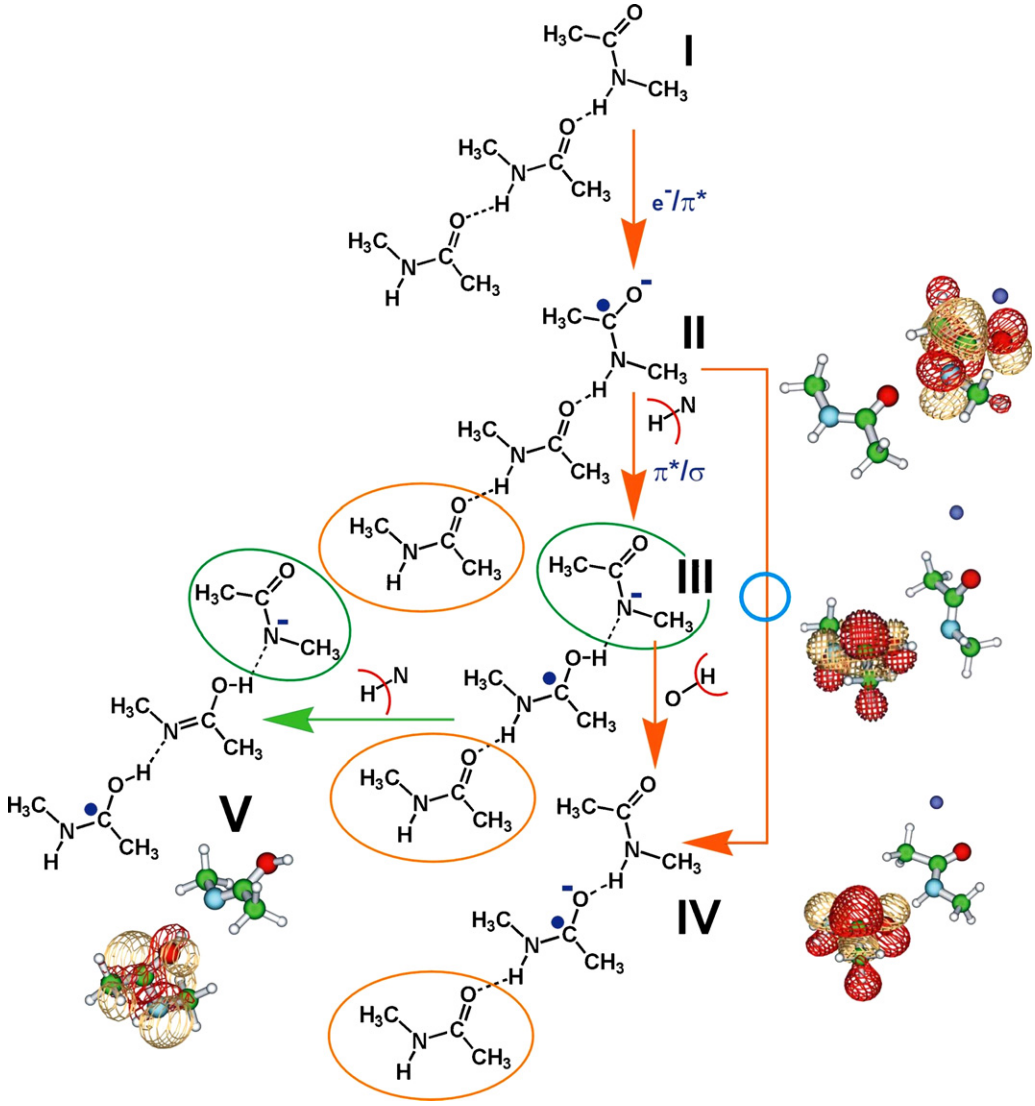

Fig. 3. Coulomb-assisted electron attachment (I → II) followed by reaction Scheme 5 (brown arrows) showing an electron in an OCN π* orbital of II followed by H atom transfer (and π* → σ electron movement) to form a •C—OH radical in III and subsequent proton transfer to form a negative •C—O⁻ radical in IV. The through-bond electron transfer variant of Scheme 5 is labeled with a blue circle. Reaction Scheme 6 (green arrow) involves H atom transfer from an H—N bond in the neutral radical center of III to the π bond of another amino acid to form a new neutral •C—OH radical in V. Also shown for each species is the orbital containing the unpaired electron.

bottom •C–OH center is deprotonated by the negative nitrogen atom to neutralize the top amino acid and generate a •C–O⁻ radical anion center on the bottom IV.

It turns out (we discovered this during our calculations) there is another route by which the •C–O⁻ radical anion center can propagate from II to IV. As the H–N bond on the upper amino acid elongates, the electron residing in the π* orbital of the top amino acid can migrate through the σ* orbital of this H–N bond directly into the π* orbital on the bottom amino acid. This through-bond electron transfer path is labeled "e⁻ transfer" in Scheme 5. Either pathway in Scheme 5 allows a negatively charged •C–O⁻ radical center to propagate along a helical chain.

The labels used to number the species in Schemes 5 and 6 have been selected to be consistent with labels assigned to these species as they appear in Figs. 3–5 where we provide quantitative data from our ab initio calculations on them.

In Scheme 6, a neutral •C–OH radical center III is propagated by homolytically cleaving an amide H–N bond, transferring this amide's H atom to the π bond of the oxygen atom of the second amino acid (to form a new •C–OH radical), while also forming a C=N π bond on the first amino acid to generate species V. Of course, the process in Scheme 6 can then propagate the neutral •C–OH radical even further down the helical chain.

Let us now consider these two propagation steps in greater detail, in particular focusing on the energy requirements and barriers associated with such anionic or neutral radical propagations.

In Fig. 3, we show a reaction diagram that is meant to represent both Schemes 5 and 6 in a more detailed manner, also showing the orbital in which the unpaired electron resides for each species. In this depiction we show three amino acids for each of species I through V to suggest the amino acids are part of a helical structure. For species II–V, one of the amino acids has a colored circle surrounding it. The brown-circled amino acids were not included in the calculations relating to the reaction connected by brown arrows, which is the reaction path shown

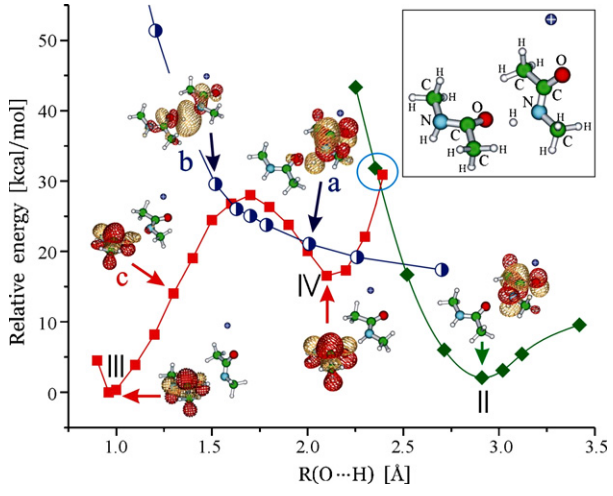

Fig. 4. MP2-level energy as a function of the distance *R* between the oxygen of the bottom carbonyl and the hydrogen migrating from the top nitrogen to the bottom oxygen for various electronic states connecting species II, III, and IV of Fig. 3.

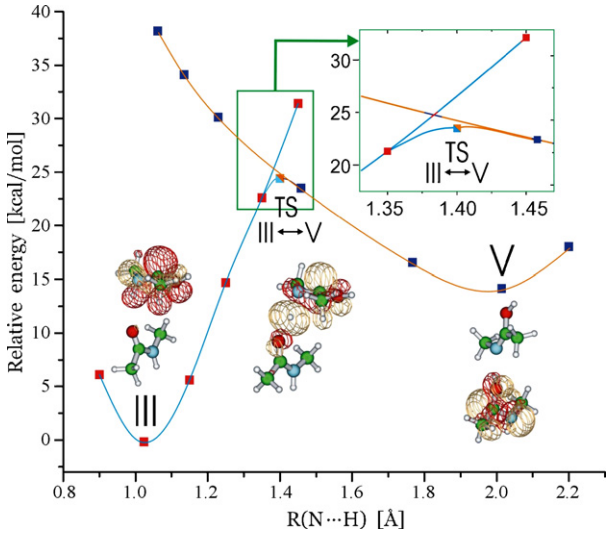

Fig. 5. MP2-level energy profile connecting species III and V in which an unpaired electron migrates from one amino acid to another without displacing the negative charge. Also shown is the orbital in which the unpaired electron resides.

in Scheme 5. The green-circled amino acids were not included in the calculations relating to the III → V reaction connected by the green arrow, which is the reaction of Scheme 6. That is, both for the brown and green reaction paths, only two alanine units were explicitly included in our ab initio calculations; the circled amino acid is shown only to remind the reader that we are attempting to characterize a chain of alanines arranged as they would be placed in a helix.

Let us first consider the reaction paths of Scheme 5 whose energy profiles are given in Fig. 4. At the top right corner of Fig. 4, we show the atomic structure of the two amino acids involved in the reaction as well as the location of the positive charge used to Coulomb-stabilize the OCN π* orbitals. These reaction paths allows the •C–O⁻ π*-attached anionic center to migrate from the first amino acid connecting species II and species IV.

The first thing to notice in Fig. 4 is that species II is ca. 16 kcal mol^{-1} more stable than species IV although both species contain an •C–O⁻ π* anionic center. This difference in energy derives largely from the fact that species I is closer to the stabilizing positive charge than is species IV; this difference in Coulomb interaction provides an energy expense to charge migration away from the positive site along the "helix".

The most straightforward path within Scheme 5 turns out to be the through-bond electron transfer path whose energy profile in Fig. 4 we now follow. Beginning as species II with the attached electron in the π* orbital of the top amino acid (this electronic state's energy variation is given by the green curve in Fig. 4), the H–N bond in II is elongated as a result of which the OH distance decreases. As the OH distance nears 2.4 Å, the attached electron evolves from the green curve (in the top amino acid's π* orbital) into the mixed π*/σ* orbital (whose energy profile is given in the blue curve) labeled "a" in Fig. 4. Subsequently, the electron moves from this π*/σ* orbital into the π* orbital of the bottom amino acid (whose energy profile is given in the red

curve) forming species IV. Along this green-to-blue-to-red path, the highest barrier that must be surmounted is ca. 20 kcal mol^{-1}.

The other path in Scheme 5 also begins on the green energy surface of species II in which the attached electron resides in the π* orbital of the top amino acid. As the N–H bond is elongated (and hence the O–H distance decreases), the attached electron again migrates into an orbital of mixed π*/σ* character (the blue curve), but the H–N distance continues to elongate until the electronic character of the blue curve becomes purely σ* orbital. This means the H–N bond is essentially broken, the nitrogen center is negatively charged, and the H atom has been released. As the H atom moves even closer to the carbonyl oxygen, it attacks the π bond, an O–H bond forms and the unpaired electron moves onto the π* orbital of the second amino acid (from the blue curve to the red curve). At this point (III) on the reaction path, one has a carbon centered radical on the second amino acid, the hydrogen atom is involved in an O–H bond on the second amino acid, and the top amino acid's nitrogen atom holds the negative charge in a lone-pair orbital. Finally, the O–H bond on the second amino acid is heterolytically cleaved allowing a proton to migrate to the top amino acid to reform the H–N bond generating species IV. Because the unpaired electron remains in the π* orbital of the bottom amino acid throughout this step, the system follows the red energy curve for this entire step. This results in a species (IV) in which the negative charge and the unpaired electron both reside on the second amino acid.

The energy profiles shown in Fig. 4 indicate that either path of Scheme 5 requires surmounting a barrier of ca. 20–25 kcal mol^{-1} and overcoming an endothermicity of ca. 16 kcal mol^{-1}. As noted earlier, much of the endothermicity derives from the fact that this path causes the negative charge of the OCN π*-attached species to move from the first to the second amino acid and thus move away from the Coulomb-stabilizing positive group. The precise value of the energy cost to such charge migration will, in any real peptide, depend on the location of the positive charge. However, the data of Fig. 4 suggest that there will be an energy barrier to be overcome to effect such a charge migration because one must displace the N–H bond sufficiently to allow the π*-attached electron to migrate from one amino acid to another.

If charge migration from one amino acid's π* orbital to another does take place, N–C_α bond cleavage within the latter amino acid could be expected to occur as we discussed in Section 4.1. Of course, the energy cost would be that of migrating the charge plus that of cleaving the N–C_α bond, so the rate of such cleavage would be considerably slower than for cleaving the N–C_α bond of the amino acid to which the electron initially attaches. Nevertheless, if charge migration and N–C_α cleavage were to occur, again the three hydrogen bonds that act to bind together the c/z$^\bullet$ fragments of such an N–C_α bond cleavage might not permit the c/z$^\bullet$ species to dissociate and be detected thus appearing to "protect" the helix-involved N–C_α bonds.

It should be noted that similar proposals involving migration of charge and/or unpaired electrons along helices have been made, for example, in [17–21] but the level of detail surrounding the potential energy profiles for such processes presented here is new.

4.3. Migration of the π*-attached electron without charge migration

Now, let us examine the path of Scheme 6 shown with a green arrow in Fig. 3 connecting species III and V, involving a migration of the $^\bullet$C–OH radical without moving the negative charge. Of course, because we assume an electron initially attaches to I to generate II, the path discussed above, in which an electron and an H atom migrates from the first to the second amino acid, must first be followed from II to generate III. As noted earlier, this step requires ca. 20–25 kcal mol^{-1}. However, once III is generated, rather than moving back "uphill" to species IV, another possibility exists. The path of Scheme 6 allowing radical propagation has the energy profile shown in Fig. 5.

This data suggest that migration of an H atom the H–N bond of the second amino acid to the third amino acid can occur to form a $^\bullet$C–OH radical on the third amino acid leaving the second amino acid in an imino (MeN=C(OH)–Me) state. However, this requires surmounting a ca. 24 kcal mol^{-1} barrier (near R_{NH} = 1.4 Å) as shown in Fig. 5 (in [3d], the Turecek group determined this barrier at a higher level of theory to be ca. 12–14 kcal mol^{-1}). This radical migration process, which is similar to that suggested by others (see [17–21]) could be expected to proceed even further along the helical chain, but each time a H atom is transferred, another barrier would have to be surmounted.

For each of the $^\bullet$C–OH radicals formed anywhere along the helix, N–C_α bond cleavage can occur by surmounting barriers of the magnitude discussed in Section 4.1. The energy cost would be that to migrate the radical and that to cleave the N–C_α bond, so it is likely that more N–C_α cleavage occurs at the amino acid to which the electron initially attaches although propagation of radicals along the helix can be expected to occur over a limited distance.

It should again be noted that Zubarev's group [17] has shown evidence for hydrogen atom migration in forming c /z$^\bullet$ fragments, McLafferty and coworkers [18] also showed evidence for H atom migration along helical turns, and Tsybin et al. has done likewise [19] as has O'Connor and coworkers [20]. In addition, Tysbin et al. [19,21] discussed the possibility of electronic excitation migration along helices. Hence, the propagation steps we are investigating here are not without precedent, but the detailed treatment of the reaction barriers involved is a new contribution here.

In summary, the energy profiles of Figs. 4 and 5 relating to the propagation steps of Schemes 5 and 6 suggest the following possibilities:

(1) Beginning with an electron attached to a Coulomb-stabilized OCN π* orbital (species II), N–C_α bond cleavage can occur at this amino acid by surmounting a 30–34 kcal mol^{-1} barrier.
(2) The attached electron and charge can propagate to the amino acid one helical turn down the chain (species IV) at a cost of ca. 20–25 kcal mol^{-1}. Then, N–C_α cleavage can occur at the latter amino acid but only after an additional 30–34 kcal mol^{-1} barrier is overcome. A significant frac-

tion of the energy difference between species II and IV derives from the difference in Coulomb interactions with the positive site and thus can vary for "real" helical peptides. However, the barriers lying between II and IV are expected to persist although their heights could vary depending on where the positive site(s) actually reside.

(3) Alternatively, an H atom can migrate from the first to the second amino acid, leaving the negative charge on the first, to generate a $^{\bullet}$C–OH radical on the second amino acid (species III) but only by surmounting a barrier that is also in the 20–25 kcal mol^{-1} range. This radical-centered amino acid can then undergo N–C$_\alpha$ cleavage by overcoming another barrier.

(4) Once a $^{\bullet}$C–OH radical is formed on the second amino acid, this radical can be propagated further down the helix (leaving behind an imino group) by surmounting a barrier of ca. 25 kcal mol^{-1} for each propagation step. This chain of propagation can be expected to be only weakly affected by the location of charges in "real" peptides because it does not involve movement of the negative charge site.

Having discussed results on model one- and two- alanine systems where the issues of hydrogen bonds holding together c/z$^{\bullet}$ fragments and propagation along helical chains arose, let us now discuss our findings for the five-alanine model.

4.4. Results on a five-alanine helix

In Fig. 6, we show the five-alanine model compound that we use to extend our study as well as the positive charge (in blue to the top left of the helix) used to Coulomb-stabilize the OCN π* orbital. Also shown is the π* orbital that the attached electron occupies. The plot shows the energy of the system as a proton transfer takes place from the second to the first amino acids changing a NCO$^-\cdots$H–N species into a NCOH$\cdots$N$^-$ species.

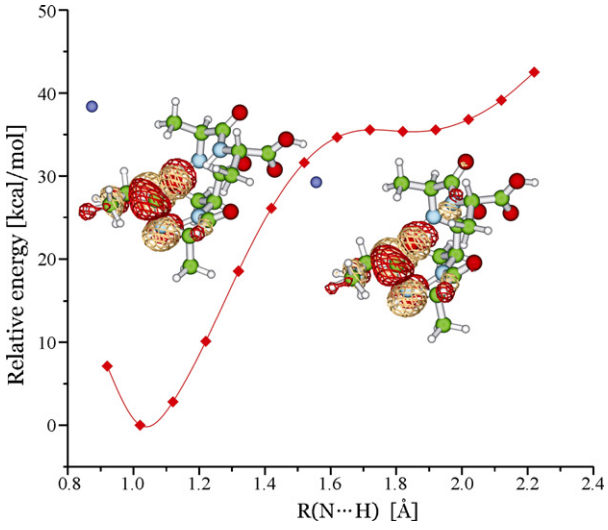

Fig. 6. Energy profile for migrating a proton from the H—N bond of the second amino acid to the negative oxygen atom of the first amino acid. Also shown is the orbital containing the unpaired electron for the O$^-\cdots$H—N species (left) and for the O—H$\cdots$N$^-$ species (right).

Clearly, as has been shown by others, the electron-attached OCN$^-$ π* system has a very large proton affinity [22]. But, so does the $^-$N-anionic center, with the result being that, in the helix geometry with the negative carbonyl oxygen atom hydrogen bonded to a neighboring H–N unit, it is considerably more favorable (by more than 30 kcal mol^{-1}) for the H–N proton to not migrate to the electron-attached OCN$^-$ site. Therefore, in the subsequent analysis of N–C$_\alpha$ bond cleavage within the five-alanine model compound, we focus on data in which the electron-attached system exists in the NCO$^-\cdots$H–N structure than in the NCO–H$\cdots$N$^-$ structure.

In the top of Fig. 7 we show the energy profile for cleaving the N–C$_\alpha$ bond of the amino acid to which an electron has been attached to form a NCO$^-\cdots$H–N structure as shown in Fig. 6. In the bottom of Fig. 7, we show a corresponding plot for cleaving the N–C$_\alpha$ bond for the NCOH$\cdots^-$N tautomer shown in Fig. 6. As in our earlier discussion of the one- and two-alanine model compounds, the plot displays two branches. One branch

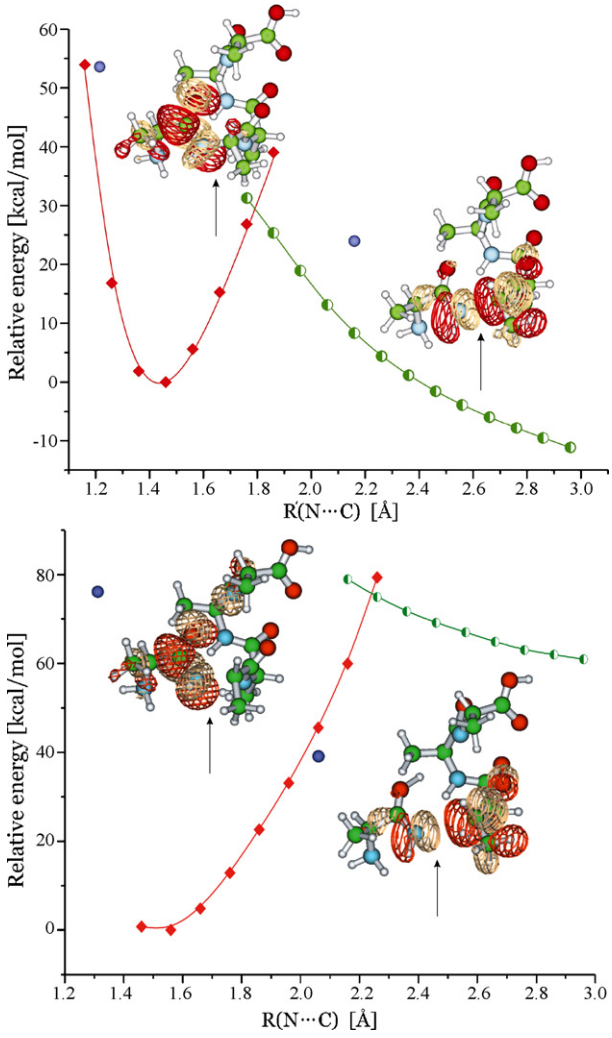

Fig. 7. MP2-level energy profiles for π*-attached (red) and σ*-attached (green) states of five-alanine helix in C–O$^-\cdots$H—N conformation (top) and in C—OH$\cdots^-$N tautomers (bottom). Also shown are the Coulomb-stabilizing positive charge, the N—C$_\alpha$ bond being stretched (arrows), and the orbital holding the attached electron.

describes the diabatic energy surface in which the attached electron resides in the π* orbital; the other branch is the diabatic surface with the electron in the N–C_α σ* orbital.

The most important observation to make in analyzing the data in the top of Fig. 7 is that the barrier (ca. 30 kcal mol^{-1}) to N–C_α cleavage, obtained from the energy at which the π* and σ curves cross, is no different from what we found in the single-alanine case regardless of whether hydrogen bonding is involved (see Fig. 2). Thus, there seems to be no difference in the barrier to N–C_α bond cleavage when the electron-attached OCN^- unit is isolated or is involved in hydrogen bonding in a helix. These data again suggest that the helix's role in "protecting" amino acids against N–C_α cleavage under ECD or ETD conditions does not arise from the helix making the N–C_α bond cleavage barrier higher than for the amino acid that is not helix-involved.

5. Speculation

It is our belief that the ab initio theoretical data presented here offer new insight into what can happen once an electron attaches (in ECD or ETD) to a Coulomb-stabilized OCN π* orbital of a helical peptide. There are, of course, accuracy limitations in our data that preclude our making quantitative absolute predictions about the rates of bond cleavage and of electron migration. However, our results suggest that radical or charge migration along helical peptides may occur at rates competitive with those for N–C_α cleavage. Moreover, when N–C_α cleavage occurs at the amino acid to which the electron initially attaches, we suggest that three hydrogen bonds hold together the c and $z^\bullet$ bond-cleavage products by ca. 26 kcal mol^{-1} (16 kcal mol^{-1} for the anion-involving bond and 5 kcal mol^{-1} for each of the other two). Indeed, our evidence suggests that it may be that the cleaved but hydrogen bonded c and $z^\bullet$ product ions are the embodiment of what has been suggested to be "protection" of helix-involved N–C_α bonds. This prediction should be amenable to experimental testing using CAD, IR excitation, or heating (following ECD or ETD).

Our suggestion that hydrogen bonds can cause nascent N–C_α cleavage products to not immediately dissociate is not new although our suggestion that an especially strong anionic hydrogen bond is involved may be. Turecek argues in [3e] that breaking hydrogen bonds between incipient c and $z^\bullet$ fragment ions can be important to consider and McLafferty and coworkers have found [23] it necessary to use subsequent collisionally activated dissociation (CAD) to dissociate c and $z^\bullet$ fragment ions formed under ECD conditions. In addition, McLuckey and coworkers [2c] have found that elevated bath temperature in ETD generates fragment c and $z^\bullet$ ions not found by ETD at lower temperature, and Cooper et al. [24] offer a nice review in which ECD/CAD methods and their outcomes are discussed in some detail. These observations are in line with our findings above. On the other hand, Zubarev and coworkers [25] have argued that involvement in hydrogen bonding can even increase the rate of N–C_α cleavage, so it is fair to say that this issue is not resolved (and thus the need for our contribution).

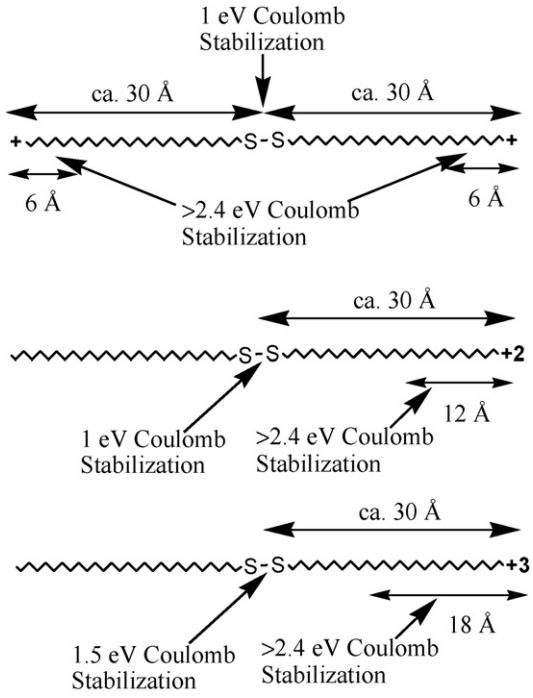

Fig. 8. Depictions of helical systems as in Fig. 1 that are +1 charged at both termini and +2 or +3 charged at only one terminus showing the total Coulomb stabilization at the SS bond. Also shown are the regions where the Coulomb stabilization should be sufficient (>2.4 eV) to render π* attachment to amide OCN units exothermic.

At this time, we also want to make other predictions, based on the Coulomb-assisted direct attachment mechanism and taking into consideration our findings here about propagation of π*-attached electrons and radical defects along the helix. In Fig. 8 we show crude depictions of model systems derivative of the $(AcCA_{10}–NH_2 + Na)_2^{2+}$ species discussed earlier. The top drawing is supposed to represent $(AcCA_{20}–NH_2 + Na)_2^{2+}$ and to show the (ca. 30 Å, assuming helical structures) distances from the sodiated termini to the S–S bond. Also shown are the distances of ca. 6 Å (obtained as [26] 14.4 eV Å/2.4 eV) within which Coulomb-assisted direct electron attachment to OCN π* orbitals would be expected to take place (and within which the data presented here suggest that N–C_α cleavage can be expected to occur). Thus, for this model compound, our findings predict that:

(a) Fragmentation of the S–S bond (via. Coulomb-assisted direct electron attachment) should occur.
(b) Cleavage of N–C_α bonds of amino acids within ca. 6 Å of the termini should occur, but
(c) The c and $z^\bullet$ products formed upon such N–C_α cleavage will, if these amino acids are helix-involved, be bound together by ca. 26 kcal mol^{-1} through hydrogen bonds. Hence, subsequent CAD may be required to detect these c and $z^\bullet$ fragments. On the other hand, if the c and $z^\bullet$ product ions resulting from cleavage within ca. 6 Å of the termini are detected, this would support the claim of [3j] that these near-terminus amino acids are not within the helical structure but are involved in "fraying".

The second model system in Fig. 8 has a +2 charge (e.g., a Mg^{+2} or Ca^{+2} cation) at one terminus and could represent $(H_2N{-}A_{20}CAcAcCA_{20}{-}NH_2 + Ca)^{2+}$, for example. Assuming the A_{20} units retain their helical character, this species will have the same Coulomb stabilization at the S–S bond site as in $(AcCA_{20}{-}NH_2 + Na)_2^{2+}$, but the distance over which attachment to OCN π* orbitals on the right half can be expected is 12 Å. We would therefore predict that S–S cleavage should occur and N–C_α cleavage should occur along the right-hand helix (perhaps requiring subsequent CAD or other means to break the three hydrogen bonds holding the c and z• fragments together to detect these fragment ions) over a distance of about 12 Å in this compound. We would also predict that N–C_α cleavage should not occur in the left-hand helix. Of course, S–S bond cleavage should also occur and in amounts similar to that in the first model compound.

The third model system (e.g., with Al^{3+} bound to one terminus instead of Ca^{2+}) would be expected to produce S–S cleavage perhaps even in greater yield than in the first two compounds (the Coulomb stabilization is larger in this species) as well as N–C_α cleavage only within the right-hand helix but over a distance of ca. 18 Å from its terminus. Again, subsequent CAD or other means would probably be required to break the three hydrogen bonds holding the c and z• fragments together to detect these fragment ions except for any near-terminus amino acids not involved in the helical structure for which N–C_α products should be readily observed.

It is possible that the latter two classes of model systems will not retain a spatially extended structure analogous to that shown in Fig. 1 because of the lack of positive charges at both Lys termini. It may, therefore, be necessary to work with species that are positively charged at both ends (e.g., $H^+ \ldots Ca^{2+}$, $H^+ \cdots Al^{3+}$, $Na^+ \cdots Ca^{2+}$). It is also possible that the di- and tri-valent cations will not simply bind to the Lys amine groups but will undergo reaction with the model peptides. Therefore, it may be necessary to find alternative means (e.g., appending two or three singly charged Lys units to the termini) to render one terminus multiply charged. It would also be worth considering using Lys units in which the $-NH_3^+$ charge is replaced by $-N(CH_3)_3^+$ to eliminate labile hydrogens. For the purposes of this paper, it probably suffices to suggest that helical poly-alanine structural units be created with charged functionalities that will allow the predictions of the Coulomb model discussed here to be further tested.

6. Summary

Ab initio electronic structure simulations have been carried out on small alanine-based fragments to which an excess electron has been added to a Coulomb-stabilized amide OCN π* orbital. The relative positioning of the fragments has been designed to model the helical environment existing, for example, in extended α-helices of poly-alanine. The primary findings and predictions resulting from these simulations are as follows:

(1) There seems to be little or no difference between the energy barriers (30–34 kcal mol^{-1}) for N–C_α bond cleavage when the carbonyl oxygen of an alanine is or is not involved in a hydrogen bond to a nearby (i.e., as in a helix) H–N bond. This suggests that involvement in the hydrogen-bonding network of a helix alone does not "protect" helix-involved amino acids from undergoing N–C_α cleavage by increasing the barrier to this cleavage.

(2) When an electron attaches to a helix-involved Coulomb-stabilized OCN π* orbital and the N–C_α bond cleaves, three hydrogen bonds act to bind together the c and z• fragment ions. One of these hydrogen bonds is especially strong (>16 kcal mol^{-1}) because it connects the negatively charged oxygen atom of the OCN unit to the H–N bond of the amino acid one turn down the helix. This leads us to predict that the c and z• fragment ions could, subsequent to ECD/ETD, be detected using CAD or other means but that ca. 26 kcal mol^{-1} (one hydrogen bond of > 16 kcal mol^{-1} and two of 5 kcal mol^{-1}) would have to be imparted to do so. This result suggests that the "protection" against N–C_α cleavage of helix-involved amino acids may result from the strong hydrogen bonding that binds the c and z• fragment ions. This conclusion is in line with what others have suggested earlier (see [2c,3e,23,24,27]) about hydrogen bonds holding c and z• together after N–C_α cleavage.

(3) When an electron attaches to a helix-involved Coulomb-stabilized OCN π* orbital, it can migrate to the π* orbital of the neighboring amino acid (i.e., that hydrogen bonded to the first within the helix) by overcoming a barrier. After migrating to a new amino acid, N–C_α cleavage can occur at the latter site. However, the energy cost for this kind of N–C_α cleavage would be 30–34 kcal mol^{-1} plus the cost to effect migration (ca. 20–25 kcal mol^{-1}).

(4) It is also possible for the hydrogen atom in the H–N bond of the amino acid to which the electron initially attaches to migrate to the oxygen atom of its helix-neighbor amino acid to form a •C–OH radical site on the latter amino acid, but at a cost of 20–25 kcal mol^{-1}. This radical center can be further propagated down the helix, but each propagation step has an energy barrier of ca. 20–25 kcal mol^{-1}. In addition, for each such •C–OH radical, N–C_α cleavage can also occur with an additional cost of 30–34 kcal mol^{-1}. Although, this barrier information is new here, the idea of H atom migration along such helices was suggested earlier in several places (see [3d,17–21] by several groups.

Although, the evidence provided here suggests that N–C_α bond cleavage in helix-involved amino acids is not really "protected" but that the c and z• fragment ions formed in such cleavages are held together by >26 kcal mol^{-1} hydrogen bonding, there is one aspect of the "protection" issue that we have not studied here. In particular, it is possible that the cross-section for electron attachment (capture or transfer) to helix-involved OCN π* orbitals is significantly smaller than that for the π* orbitals of amino acids not involved in helices. Because our expertise does not include electron–molecule scattering, we must leave it to others to examine this possibility. We suggest to other workers that such a study would be timely and could provide important additional insight about the issue of "protection".

In addition to these conclusions and predictions, we have put forth here several speculations relating to model compounds similar to those used in [3j]. In particular, we offered concrete predictions about the S–S and N–C_α cleavage that would be expected to occur in $(AcCA_{20}–NH_2 + Na)_2^{2+}$, $(H_2N–A_{20}CAcAcCA_{20}–NH_2 + Ca)^{2+}$, and $(H_2N–A_{20}CAcAcCA_{20}–NH_2 + Al)^{3+}$ and analogous species. In all three model compounds, efficient S–S bond cleavage is predicted. In $(AcCA_{20}–NH_2 + Na)_2^{2+}$ N–C_α cleavage is predicted to occur within ca. 6 Å of either terminus. For $(H_2N–A_{20}CAcAcCA_{20}–NH_2 + Ca)^{2+}$, the N–$C_\alpha$ cleavage should occur over a range of ca. 12 Å from the positively charged terminus but not elsewhere. Finally, for $(H_2N–A_{20}CAcAcCA_{20}–NH_2 + Al)^{3+}$, the N–$C_\alpha$ cleavage should range up to 18 Å from the positively charged terminus but not elsewhere. In the event that amino acids undergoing N–C_α cleavage are helix-involved, it may require subsequent CAD or other energizing means to detect the c and $z^\bullet$ fragments. It is our hope that the predictions and speculations offered here could soon be put to experimental test so that further insight into the mechanisms of electron-attachment-induced peptide fragmentation can be better understood.

Acknowledgements

We thank the three referees for many very helpful comments. This work has been supported by NSF Grant No. 0240387 to J.S. Significant computer time provided by the Center for High Performance Computing at the University of Utah is also gratefully acknowledged. We dedicate this paper to the infant Michal Myslinski, Jr. who successfully fought for his life as the research reported here was carried out.

References

[1] (a) R.A. Zubarev, N.L. Kelleher, F.W. McLafferty, J. Am. Chem. Soc. 120 (1998) 3265;
(b) R.A. Zubarev, N.A. Kruger, E.K. Fridriksson, M.A. Lewis, D.M. Horn, B.K. Carpenter, F.W. McLafferty, J. Am. Chem. Soc. 121 (1999) 2857;
(c) R.A. Zubarev, D.M. Horn, E.K. Fridriksson, N.L. Kelleher, N.A. Kruger, M.A. Lewis, B.K. Carpenter, F.W. McLafferty, Anal. Chem. 72 (2000) 563;
(d) R.A. Zubarev, K.F. Haselmann, B. Budnik, F. Kjeldsen, F. Jensen, Eur. J. Mass Spectrom. 8 (2002) 337.

[2] (a) J.E.P. Syka, J.J. Coon, M.J. Schroeder, J. Shabanowitz, D.F. Hunt, Proc. Natl. Acad. Sci. U.S.A. 101 (2004) 9523;
(b) J.J. Coon, J.E.P. Syka, J.C. Schwartz, J. Shabanowitz, D.F. Hunt, Inter. J. Mass Spectrom. 236 (2004) 33;
(c) S.J. Pitteri, P.A. Chrisman, S.A. McLuckey, Anal. Chem. 77 (2005) 5662;
(d) H.P. Gunawardena, M. He, P.A. Chrisman, S.J. Pitteri, J.M. Hogan, B.D.M. Hodges, S.A. McLuckey, J. Am. Chem. Soc. 127 (2005) 12627.

[3] (a) E.A. Syrstad, F. Turecek, J. Phys. Chem. A105 (2001) 11144;
(b) F. Turecek, E.A. Syrstad, J. Am. Chem. Soc. 125 (2003) 3353–3369;
(c) F. Turecek, M. Polasek, A. Frank, M. Sadilek, J. Am. Chem. Soc. 122 (2000) 2361;
(d) E.A. Syrstad, D.D. Stephens, F. Turecek, J. Phys. Chem. A107 (2003) 115;
(e) F. Turecek, J. Am. Chem. Soc. 125 (2003) 5954;
(f) E.A. Syrstad, F. Turecek, Am. Soc. Mass Spectrom. 16 (2005) 208;
(g) E. Uggerud, Inter. J. Mass. Spectrom. 234 (2004) 45;
(h) I. Anusiewicz, J. Berdys-Kochanska, J. Simons, J. Phys. Chem. A109 (2005) 5801;
(i) I. Anusiewicz, J. Berdys-Kochanska, P. Skurski, J. Simons, J. Phys. Chem. A110 (2006) 1261;
(j) A. Sawicka, P. Skurski, R.R. Hudgins, J. Simons, J. Phys. Chem. B107 (2003) 13505;
(k) M. Sobczyk, P. Skurski, J. Simons, Adv. Quantum Chem. 48 (2005) 239;
(l) A. Sawicka, J. Berdys-Kochaska, P. Skurski, J. Simons, Inter. J. Quantum Chem. 102 (2005) 838;
(m) I. Anusiewicz, J. Berdys, M. Sobczyk, A. Sawicka, P. Skurski, J. Simons, J. Phys. Chem. A109 (2005) 250;
(n) V. Bakken, T. Helgaker, E. Uggerud, Eur. J. Mass Spectrom. 10 (2004) 625.

[4] This energy can be estimated by using the formula 14.4 eV Å/R(Å) where R is the distance in Å from a positive site to the orbital being stabilized. Of course in real systems (e.g., containing $–N(CH_3)_3^+$) the positive charge may be somewhat delocalized so a computation of the Coulomb potential using the location of one atom (e.g., the N atom) to define the distance R can be expected to give only a qualitative estimate.

[5] C. Dezarnaud-Dandine, F. Bournel, M. Troncy, D. Jones, A. Modelli, J. Phys. B: At. Mol. Opt. Phys. 31 (1998) L497;
M. Seydou, A. Modelli, B. Lucas, K. Konate, C. Desfrancois, J.P. Schermann, Eur. Phys. J. D 35 (2005) 199.

[6] (a) M. Sobczyk, J. Simons, J. Phys. Chem. B 110 (2006) 7519;
(b) M. Sobczyk, J. Simons, Inter. J. Mass. Spectrom. 253 (2006) 274.

[7] This R^{-2} dependence relates to the fraction of the surface of a sphere of radius R that overlaps the OCN π^* or SS σ^* orbital a distance R away.

[8] When more than one positive site is present, one must use the sum of such factors to evaluate the Coulomb potential.

[9] (a) The workers of Ref. [3j] cite the following reference in support of this claim: R.R. Hudgins, M.F. Jarrold, J. Am. Chem. Soc. 121 (1999) 3494, In this paper, a singly-charged anlog of the species shown in Fig. 1 was used and found to display extended rather than compact structure, suggesting that the doubly-charged species would also be extended because it would also have internal Coulomb repulsion between the two positive Lys sites;
(b) A more recent effort aimed at using mobility measurements to probe extended and more compact structures of alanine-containing peptides is given in: A.E. Counterman, D.E. Clemmer, J. Phys. Chem. B 107 (2003) 2111.

[10] The rate of exponential decay we found for the through-bond electron transfer process in Ref. [3b] pertained to electron migration through $–CH_2–$ methylene units. It might be that the rate of migration along peptide backbones, where both σ and π bonds occur, is significantly faster. We are in the process of considering this possibility at present.

[11] In Ref. [6b], we found the exponential decay of the through-bond electron transfer matrix elements H1, 2 = A exp(−βR) for the ground- and excited-Rydberg states to vary with $\beta = 1.18\ Å^{-1}$ and $\beta = 0.68\ Å^{-1}$, respectively. So, for two sites 32 Å apart, the exp(−βR) factor would be expected to be 10^{-10} or smaller, essentially ruling out the TBET mechanism for the case under discussion. We note that these β parameters are not out of line with what one observes in other through-bond electron transfer processes. See, for example: H.M. McConnell, J. Chem. Phys. 35 (1961) 508;
R. Hoffmann, Acc. Chem. Res. 4 (1971) 1;
M.D. Newton, Inter. J. Quantum Chem. 77 (2000) 255;
K.D. Jordan, M.N. Paddon-Row, Chem. Rev. 92 (1992) 395;
B.P. Paulson, L.A. Curtiss, B. Bal, G.L. Closs, J.R. Miller, J. Am. Chem. Soc. 118 (1996) 378.

[12] R. Hudgins, K. Håkansson, J.P. Quinn, C.L. Hendrickson, A.G. Marshall, Proceedings of the 50th ASMS Conference on Mass Spectrometry and Allied Topics, Orlando, Florida, June 2–6, 2002.
A020420. Fig. 1 first appears in publication in Ref. [3j]. In Ref. [9] another depiction of this kind of extended helical structure appears.

[13] (a) A.D. McLean, G.S. Chandler, J. Chem. Phys. 72 (1980) 5639;
(b) R. Krishnan, J.S. Binkley, R. Seeger, J.A. Pople, J. Chem. Phys. 72 (1980) 650.

[14] M.J. Frisch, G.W. Trucks, H.B. Schlegel, G.E. Scuseria, M.A. Robb, J.R. Cheeseman, J.A. Montgomery Jr., T. Vreven, K.N. Kudin, J.C. Burant, J.M. Millam, S.S. Iyengar, J. Tomasi, V. Barone, B. Mennucci, M. Cossi, G. Scalmani, N. Rega, G.A. Petersson, H. Nakatsuji, M. Hada, M. Ehara,

K. Toyota, R. Fukuda, J. Hasegawa, M. Ishida, T. Nakajima, Y. Honda, O. Kitao, H. Nakai, M. Klene, X. Li, J.E. Knox, H.P. Hratchian, J.B. Cross, V. Bakken, C. Adamo, J. Jaramillo, R. Gomperts, R.E. Stratmann, O. Yazyev, A.J. Austin, R. Cammi, C. Pomelli, J.W. Ochterski, P.Y. Ayala, K. Morokuma, G.A. Voth, P. Salvador, J.J. Dannenberg, V.G. Zakrzewski, S. Dapprich, A.D. Daniels, M.C. Strain, O. Farkas, D.K. Malick, A.D. Rabuck, K. Raghavachari, J.B. Foresman, J.V. Ortiz, Q. Cui, A.G. Baboul, S. Clifford, J. Cioslowski, B.B. Stefanov, G. Liu, A. Liashenko, P. Piskorz, I. Komaromi, R.L. Martin, D.J. Fox, T. Keith, M.A. Al-Laham, C.Y. Peng, A. Nanayakkara, M. Challacombe, P.M.W. Gill, B. Johnson, W. Chen, M.W. Wong, C. Gonzalez, J.A. Pople, Gaussian 03, Revision A 1, Gaussian, Inc., Wallingford, CT, 2004.

[15] G. Schaftenaar, J.H. Noordik, J. Comput. Aided Mol. Des. 14 (2000) 123.

[16] See Table 1 in Ref. [3e].

[17] M.M. Savitski, F. Kjeldsen, M.L. Nielsen, R.A. Zubarev, J. Am. Soc. Mass. Spectom. 18 (2007) 113.

[18] K. Breuker, H. Oh, C. Lin, B.K. Carpenter, F.W. McLafferty, Proc. Natl. Acad. Sci. U.S.A. 101 (2004) 14011.

[19] Y.O. Tsybin, M.R. Emmett, C.L. Hendrickson, O.Y. Tsybin, A.G. Marshall, Am. Soc. Mass Spectrom. (2006) (abstract).

[20] N. Leymarie, C.E. Costello, P.B. O'Connor, J. Am. Chem. Soc. 125 (2003) 8949.

[21] Y.O. Tsybin, O.Y. Tysbin, P.D. Grigoriev, M.R. Emmett, C.L. Hendrickson, A.G. Marshall, Inter. Mass Spectrom. Confer. (2006) (abstract).

[22] In Ref. [3][3f] it was noted (for the first time to our knowledge) that the electron-attached OCN− moiety has a very high proton affinity (as high as 300 kcal mol−1), so it can abstract a proton from any protonated amino acid residue. However, to abstract a proton from the H─N backbone bond that belongs to the amino acid to which the electron-attached amino acid is hydrogen bonded requires even more than 310 kcal mol−1. For this reason, the helix-involved electron-attached OCN units remain in the NCO−···H─N state rather than moving to the NCO–H···N− state (2000).

[23] D.M. Horn, K. Breuker, A.J. Frank, F.W. McLafferty, J. Am. Chem. Soc. 123 (2001) 9792;
D.M. Horn, Y. Ge, F.W. McLafferty, Anal. Chem. 72 (2000) 4778.

[24] H.J. Cooper, K. Håkansson, A.G. Marshall, Mass Spectrom. Rev. 24 (2005) 201.

[25] A. Patriksson, C. Adams, F. Kjeldsen, J. Raber, D. van der Spoel, R.A. Zubarev, Inter. J. Mass Spec. 248 (2006) 124.

[26] We know that amide OCN π*-attached anion states lies vertically ca. 2.4 eV above the parent neutral. See, for example: M. Seydou, A. Modelli, B. Lucas, K. Konate, C. Desfrancois, J.P. Schermann, Eur. Phys. J. D 35 (2005) 199–205, In making this distance estimate, we consider only the Coulomb potential of the closest Na^+ ion; the effect of the more distant Na^+ ion will be minor for amino acids near the C-termini.

[27] C. Lin, J.J. Cournoyer, P.B. O'Connor, J. Am. Soc. Mass Spectrom. 17 (2006) 1605.